

# Examining the Use of Temporal-Difference Incremental Delta-Bar-Delta for Real-World Predictive Knowledge Architectures

Johannes Günther<sup>1,\*</sup>, Nadia M. Ady<sup>1</sup>, Alex Kearney<sup>1</sup>,  
Michael R. Dawson<sup>2</sup> and Patrick M. Pilarski<sup>1,2</sup>

<sup>1</sup>Department of Computing Science, University of Alberta, Edmonton, Alberta, Canada <sup>2</sup>Department of Medicine, University of Alberta, Edmonton, Alberta, Canada

Correspondence\*:  
Johannes Günther  
gunther@ualberta.ca

## ABSTRACT

Predictions and predictive knowledge have seen recent success in improving not only robot control but also other applications ranging from industrial process control to rehabilitation. A property that makes these predictive approaches well suited for robotics is that they can be learned online and incrementally through interaction with the environment. However, a remaining challenge for many prediction-learning approaches is an appropriate choice of prediction-learning parameters, especially parameters that control the magnitude of a learning machine's updates to its predictions (the *learning rate* or *step size*). To begin to address this challenge, we examine the use of online step-size adaptation using a sensor-rich robotic arm. Our method of choice, Temporal-Difference Incremental Delta-Bar-Delta (TIDBD), learns and adapts step sizes on a feature level; importantly, TIDBD allows step-size tuning and representation learning to occur at the same time. We show that TIDBD is a practical alternative for classic Temporal-Difference (TD) learning via an extensive parameter search. Both approaches perform comparably in terms of predicting future aspects of a robotic data stream. Furthermore, the use of a step-size adaptation method like TIDBD appears to allow a system to automatically detect and characterize common sensor failures in a robotic application. Together, these results promise to improve the ability of robotic devices to learn from interactions with their environments in a robust way, providing key capabilities for autonomous agents and robots.

**Keywords:** Continual Learning; Reinforcement Learning; Robot learning, Long-term autonomy, Prediction

## 1 PREDICTIVE KNOWLEDGE FOR ROBOTICS

Autonomous agents in the real world face many challenges when interacting with and learning from the environment around them, especially if they are deployed for extended periods of time. As the real world is non-stationary and complex, many of the challenges facing a deployed agent cannot be completely foreseen by its designers in advance. An agent should therefore construct its understanding of the environment using an approach that is continuous and independent, so it is empowered to adapt to its environment without human assistance.

Predictive knowledge (Sutton et al., 2011; White, 2015) is such an approach, and allows autonomous agents to incrementally construct knowledge of the environment purely through interaction (Drescher, 1991; Ring, 1994). In a predictive knowledge architecture, the environment is modelled as a set of forecasts about how signals of interest will behave. As an agent's actions have an effect on the environment, these forecasts about what will happen next are made with consideration to a policy of agent behaviour (*nexting*, as described by Modayil et al. (2014)). In this way, these predictions can capture forward-looking aspects of the environment such as, “If I continue moving my arm to the right, how much load do I expect my elbow servo to experience?” For a concrete example of predictions being used to support robot control, we consider the idea of Pavlovian control, as defined by Modayil and Sutton (2014), wherein learned predictions about what will happen next are mapped in pre-defined or fixed ways to changes in a system's control behaviours. As a principal case study, Modayil and Sutton (2014) showed how a sensor-limited robot could use a learned prediction about an impending collision to take evasive action and reduce strain on its motors *before* a collision actually occurred. Without using predictions to alter actions, a collision would need to occur before the robot would be able to take action in response to it.

Detailed demonstrations of other potential of predictive knowledge architectures in real-world domains have been offered in industrial laser welding (Günther et al., 2016), robot navigation (Kahn et al., 2018), animal models of partial paralysis (Dalrymple et al., 2018), and artificial limbs (Pilarski et al., 2013; Sherstan et al., 2015; Edwards et al., 2016; Pilarski et al., 2017). Recently, work has focused on using predictive knowledge to construct representations of state that capture aspects of the environment that cannot be described by current observations alone (Schlegel et al., 2018), and on accelerating the learning of predictive knowledge through use of successor representations (Sherstan et al., 2018).

From a computational perspective, there is strong evidence that a predictive knowledge architecture is feasible at scale. Many predictions can be simultaneously made and learned online, incrementally (Sutton et al., 2011), as a system is interacting with the environment, using methods such as temporal-difference (TD) learning (Sutton, 1988) and other standard learning algorithms from the field of reinforcement learning. Predictive knowledge architectures have been demonstrated to scale well (White, 2015) and to allow real-time learning (Modayil et al., 2014; White, 2015).

Although research to date has comprehensively established how an agent can utilize prediction learning in a broad range of environments, it is important to note that in all these previous examples, the algorithm for learning is fixed before deployment and does not itself change during learning. Specifically, the step sizes (learning rates) used by the learning algorithms in existing studies are hand-selected in advance by the experimenters through large parameter sweeps or empirical tuning. In addition to the impracticality of hand-selecting learning algorithm parameters, using a predefined and fixed step size for the lifetime of an agent might in fact significantly limit the learning capability of the agent.

It is natural to expect that the learning rate of a long-lived agent will change over time. The process of destabilizing memories and making them prone to change is observed in mammals (Sinclair and Barense, 2018) and is analogous to a temporary increase in learning rates in an autonomous agent. Following this idea, recent research has investigated approaches capable of online step-size adaptation (Mahmood et al., 2012; Sutton, 1992), wherein a learning agent is able to self-tune the size of the learning steps it takes in response to the errors observed during its own learning process. However, the aforementioned step-size adaptation methods still use a single step size for all inputs and therefore treat all inputs to a learning agent equally. Not surprisingly, the reliability and variability of different inputs can play a large role in an agent's ability to learn about future outcomes—inputs are not all created equal in terms of their utility for a

learning agent. The use of a single scalar step size therefore limits an agent’s ability to adapt to and learn more about interesting inputs and to learn less about uninteresting or noisy inputs.

By implementing an individual step size for each input to a learning agent, it is possible for an agent to treat different inputs differently during learning. One extension of scalar step-size adaptation methods to a non-scalar form is Temporal-Difference Incremental Delta-Bar-Delta (TIDBD) (Kearney et al., 2019). In their introduction of TIDBD, Kearney et al. (2019) investigated adaptation of vector step sizes on a feature level, comparing how TIDBD adapts the step sizes for noisy features versus prediction-relevant features. In this work, we translate TIDBD to a more realistic setting. Rather than investigating deteriorating features, we investigate deteriorating sensors; we consider the case where a set of sensors freezes or becomes noise, preventing perception of a useful signal. Such a situation rarely translates cleanly to a simple set of unrelated feature noise in the feature representation. Kearney et al. found in their experiments that TIDBD could outperform TD methods that lack step-size adaptation. A meta-learning method that can perform comparably to, or outperform, classic TD, yet avoid the need for time- and labour-intensive parameter tuning, is one main component for making predictive architectures practical in real-world applications. As an extension of the work done by Kearney et al. (2019), we compare TIDBD against TD methods on a robot data stream with far more parallel signals than any prior test domains. In addition, we consider the viability of TIDBD on this complex data in terms of computation and memory.

As main contributions of this work, we provide deeper understanding and intuition about the effect that using TIDBD will have on prediction-learning tasks involving complex, real-world data. In what follows, we demonstrate how TIDBD adapts the step sizes in TD learning when confronted with a non-stationary environment. By examining the operation of TIDBD in comparison to classic TD and its ability to perform feature selection in relation to specific signals in the robotic arm, this work carves out insight that will help others design persistent agents capable of long-term autonomous operation and learning.

## 2 PREDICTION-LEARNING METHODS

Key to the construction of predictive knowledge systems is the way predictions are specified. One proposal is to express world knowledge as a collection of General Value Functions (GVFs) (Sutton et al., 2011). Interaction with the world is described sequentially, where at each time step  $t$ , an agent takes an action  $A_t \in \mathcal{A}$ , which causes a transition from  $S_t$  to  $S_{t+1} \in \mathcal{S}$  specified by a Markov Decision Process. The agent’s choice of action,  $A_t$ , is determined by a probability function  $\pi : \mathcal{S} \times \mathcal{A} \rightarrow [0, 1]$ , known as a *policy*. We model our world by forming predictive questions about our sensations, which we phrase as GVFs—predictions about a signal of interest,  $C$ , from the environment over some time-scale or horizon,  $\gamma \geq 0$ , and some behaviour policy  $\pi$ . The discounted future sum of the *cumulant*,  $C$ , is known as the *return*,  $G_t = \sum_{k=0}^{\infty} \gamma^k C_{t+k+1}$ . A GVF,  $V$ , is the expected discounted return of this cumulant:  $V(s; \pi, \gamma, C) = \mathbb{E}[G_t | S_t = s]$ , which can be estimated using incremental online learning methods, such as TD learning (Sutton and Barto, 2018).

In complex domains, such as the robotics domain we explore in this paper, the state space can be large or infinite: we must use function approximation to represent GVFs. We use selective Kanerva coding, a feature construction method shown by Travník (2018) to be less sensitive to the curse of dimensionality than tile coding, yet still offering linear complexity. As our state space has 108 dimensions, this is an important advantage. Selective Kanerva coding represents the state space with a number of *prototypes*, points randomly distributed throughout the true state space. A state (point in this space) is then represented by a constant number of the closest prototypes, providing a binary feature vector indexed by the prototypes.

When performing TD learning with linear function approximation, we estimate the value  $V(s)$  as the dot product of a weight vector  $\mathbf{w}$  with a feature vector  $\mathbf{x}(s)$ , used as the state representation of  $s$ . We improve our estimate  $\mathbf{w}^\top \mathbf{x}(s)$  of  $V(s)$  through gradient descent in the direction of a TD error  $\delta_t = C_{t+1} + \gamma V(S_{t+1}) - V(S_t)$  (Algorithm 1, Line 3). The weights,  $\mathbf{w}$ , for each GVF learner are updated on each time step. A collection of GVF learners is called a *Horde* (Sutton et al., 2011).

## 2.1 AutoStep TIDBD

A challenge for modelling the world with GVFs is choosing learning parameters and selecting appropriate features to construct state with. When instantiating a set of GVFs, one must choose an appropriate step size  $\alpha > 0$  and a feature representation  $\mathbf{x}(s)$  suitable for each individual prediction. While there are demonstrations that many simultaneous GVFs can be learned using a single, shared representation (Modayil et al., 2014; White, 2015, pp. 61-78), no single step size will be appropriate for all predictions one may choose to make, and no representation will be equally suitable for all predictions; by exclusively using shared learning parameters and representations, a portion of the predictions will be at a disadvantage. For these reasons, it is desirable to tune both the step size and the representations for each individual prediction in a Horde. One method of achieving this is by using AutoStep TIDBD (Algorithm 1, adapted from Kearney et al., 2019), a step-size adaptation method for TD learning, which we hereafter simply refer to as TIDBD.

TIDBD adjusts a vector of many step sizes—one step size for each feature such that for a binary feature vector  $\mathbf{x}(s) \in \mathbb{R}^n$ , there is a vector of learned step sizes  $\alpha \in \mathbb{R}^n$ , where  $n$  is the number of features. By adapting step sizes on a per-feature basis, we are able to tune them based on their relevance; features which are highly correlated to the prediction problem should be given large step sizes, while irrelevant features should contribute less to updates and be given smaller step sizes.

---

### Algorithm 1 TD( $\lambda$ ) with AutoStep TIDBD( $\lambda$ )

---

- 1: Initialize vectors  $\mathbf{h} = 0^n$ ,  $\mathbf{z} = 0^n$ , and both  $\mathbf{w} \in \mathbb{R}^n$  and  $\beta \in \mathbb{R}^n$  as desired, and set  $\alpha_i = e^{\beta_i}$  for each element  $i = 1, 2, \dots, n$ ; initialize a scalar,  $\theta > 0$ ; observe state  $S_t$
  - 2: Repeat for each observation  $S_{t+1}$  and cumulant  $C$ :
  - 3:   Construct feature representation with  $x_i(S_t)$  as  $i$ th element of  $\mathbf{x}(S_t)$  for each element  $i = 1, \dots, n$
  - 4:    $\delta \leftarrow C + \gamma \mathbf{w}^\top \mathbf{x}(S_{t+1}) - \mathbf{w}^\top \mathbf{x}(S_t)$
  - 5:   For element  $i = 1, 2, \dots, n$ :
  - 6:      $\xi_i \leftarrow \max($
  - 7:        $|\delta[\gamma x_i(S_{t+1}) - x_i(S_t)]h_i|,$
  - 8:        $\xi_i - \frac{1}{\tau} \alpha_i [\gamma x_i(S_{t+1}) - x_i(S_t)] z_i [|\delta x_i(S_t) h_i| - \xi_i]$
  - 9:      $)$
  - 10:     $\beta_i \leftarrow \beta_i - \theta \frac{1}{\xi_i} \delta [\gamma x_i(S_{t+1}) - x_i(S_t)] h_i$
  - 11:     $M \leftarrow \max(-e^{\beta} [\gamma \mathbf{x}(S_{t+1}) - \mathbf{x}(S_t)]^\top \mathbf{z}, 1)$
  - 12:    For element  $i = 1, 2, \dots, n$ :
  - 13:      $\beta_i \leftarrow \beta_i - \log(M)$
  - 14:      $\alpha_i \leftarrow e^{\beta_i}$
  - 15:      $z_i \leftarrow z_i \gamma \lambda + x_i(S_t)$
  - 16:      $w_i \leftarrow w_i + \alpha_i \delta z_i$
  - 17:      $h_i \leftarrow h_i \max(1 + \alpha_i z_i [\gamma x_i(S_{t+1}) - x_i(S_t)], 0) + \alpha_i \delta z_i$
  - 18:     $s \leftarrow S_{t+1}$
- 

TIDBD adapts the vector step size  $\alpha$  incrementally through stochastic meta-descent over a set of meta-weights  $\beta \in \mathbb{R}^n$  to minimize the squared TD error. The meta-weights  $\beta$  are updated each time step (line



**Figure 1.** The Modular Prosthetic Limb (MPL), a robot arm with many degrees of freedom and sensors used for the experiments in this work.

10), scaled by the meta step size  $\theta$ . The memory vector  $\mathbf{h} \in \mathbb{R}^n$  is a decaying trace of updates to the meta-weights (line 16).

While TIDBD introduces the additional parameter  $\theta$ , it is insensitive to meta step sizes values, with  $\theta = 10^{-2}$  being a good choice over a variety of different prediction problems (Kearney et al., 2019).

### 3 EXPERIMENTAL SETUP

We gathered the data for our experiments from the Modular Prosthetic Limb (MPL v3) (Bridges et al., 2011)—a state-of-the-art bionic limb capable of human-like movements which can be seen in Figure 1. The MPL includes 26 articulated joints in its shoulder, elbow, wrist, and hand. It provides 17 degrees of freedom. Each motor has sensors for load, position, temperature, and current; each fingertip is outfitted with a 3-axis accelerometer and with 14 pressure pad sensor arrays. Together, these provide a data stream of 108 real-valued sensor readings that is shown in Figure 2.

Experiments by Pilarski et al. (2013) suggest that real-time prediction learning can make the control of artificial limbs more intuitive for the user. In particular, anticipation and adaptation are highly important given the world and tasks encountered by a prosthetic limb are continuously changing. Therefore, the arm is an interesting showpiece as an autonomous learner (Pilarski et al., 2017).

The architecture of our autonomous learning system was a Horde of 108 predictions: one prediction for each of the perceived sensor values. The sensor readings were the cumulants for the predictions. Both classic TD and TIDBD are online methods for estimating general value functions, meaning they predict the return based on only information observed up to the time step they are estimating the value for.

The sensor readings were also normalized and fed into the Kanerva coder to obtain feature vector  $\mathbf{x}(s)$ . The active features were selected based on their Euclidean distance from the normalized sensor reading. This feature vector was used as state representation for the Horde. For each prediction, we used a discount rate of  $\gamma = 0.9$ . This discount rate can be thought of as resulting in a 10-step time scale, because it refers

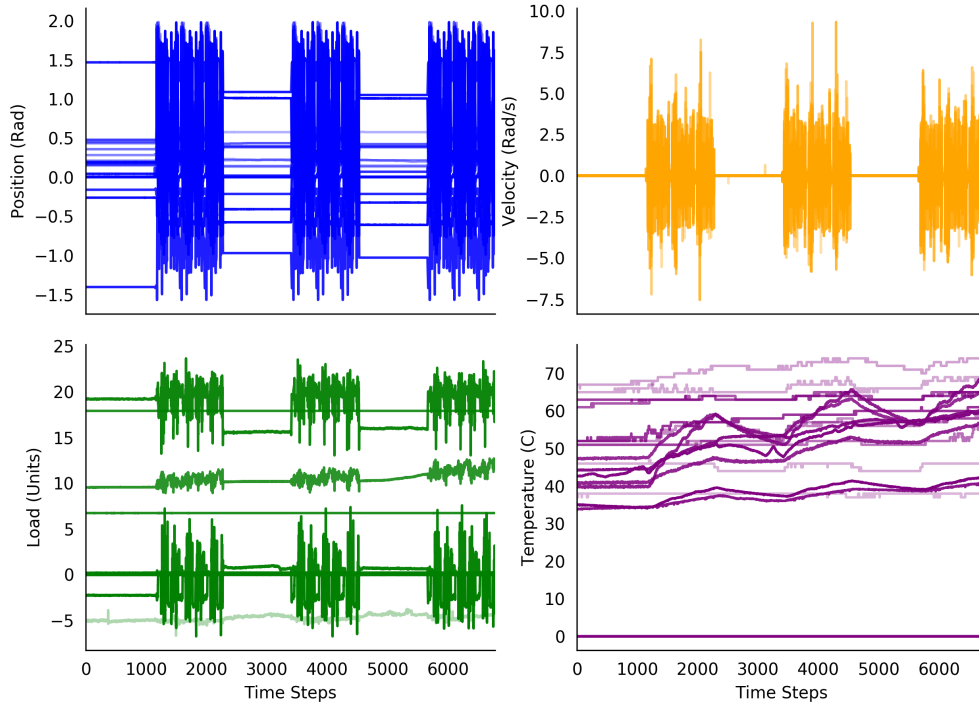


**Figure 2.** Decoded percept data from the robot over the 30 minutes of the experiment. The periods of the arm resting and the periods of the arm moving are clearly distinguishable for the position, velocity and load sensors. The values of the temperature sensors increase over the experiment, with additional increases during the periods of movement.

to, in expectation, the sum of the cumulant over 10 time steps. Succeeding time steps were 0.265s apart, on average, so a 10-step time scale refers to 2.65s. This value is potentially well suited to capturing some comparatively slow movements, e.g. the elbow extension or flexion, but might result in averaging over very fast movements, e.g. a fast grasping movement. As the computations for the predictions and return were undertaken offline—though the computations for the predictions used online methods—the computation time did not affect the length of the time step.

We measured the performance of TIDBD through a comparison with classic TD. In particular, we considered the root mean squared error (RMSE), which is essentially a measurement of the difference between the true return and the value (the expected value of the return). We computed the RMSE over all predictions for a single time step,  $t$ , as follows.

$$RMSE_t = \sqrt{\frac{\sum_{i=1}^{108} \left( \frac{G_t^{(i)} - \mathbf{x}(s_t)^\top \mathbf{w}_t^{(i)}}{|G_t^{(i)}|} \right)^2}{108}} \quad (1)$$

The superscript  $(i)$  denotes association with the  $i$ th prediction of 108. Normalization (division of the return and value estimate by  $|G_t^{(i)}|$ ) was done to make the RMSE meaningful, as the returns (and associated predictions) for different sensors were on different scales. Note that it would be unlikely for the RMSE to

reach zero. While the return was computed taking all sensor readings for the full experiment into account, both classic TD and TIDBD used only sensor readings up to the present time step. These observations do not provide enough information to perfectly predict the future.

For an meaningful comparison of classic TD with TIDBD, the parameters needed to be carefully tuned. The best parameters were chosen based on minimizing the RMSE over all predictions, summed over all time steps of the experiment. We therefore performed parameter sweeps for the number  $n$  of prototypes in the Kanerva coder, the ratio  $\eta$  of active prototypes to the total number of prototypes, and for the scalar step sizes  $\alpha$  for each prediction for classic TD. The candidates for each parameter are shown in Table 1. The candidates for  $n$ , the number of prototypes, were chosen based on the recommendations provided by Travník and Pilarski (2017). We used a full factorial experimental setup, resulting in 264 different parameter settings for the experiments with a fixed step size, those for classic TD. Because the TIDBD experiments did not require a sweep over potential step sizes  $\alpha$ , there were only 24 different parameter settings for the TIDBD experiments (accounting for candidates for  $\eta$  and  $n$ ). In total, we conducted 288 different experiments for our comparison of TD learning and TIDBD.

Parameter	Count	Candidates
$n$	4	10000, 20000, 30000, 40000
$\eta$	6	0.001, 0.002, 0.004, 0.008, 0.016, 0.032
$\alpha$	11	$\frac{0.001}{n \cdot \eta}$ , $\frac{0.002}{n \cdot \eta}$ , $\frac{0.004}{n \cdot \eta}$ , $\frac{0.008}{n \cdot \eta}$ , $\frac{0.016}{n \cdot \eta}$ , $\frac{0.032}{n \cdot \eta}$ , $\frac{0.064}{n \cdot \eta}$ , $\frac{0.128}{n \cdot \eta}$ , $\frac{0.256}{n \cdot \eta}$ , $\frac{0.512}{n \cdot \eta}$ , $\frac{1.024}{n \cdot \eta}$

**Table 1.** Parameter candidates tested in full factorial design.

To set the parameters for classic TD, the experiment was first run with a fixed step size shared by all GVFs in the Horde. In these experiments, using  $n = 30000$  and  $\eta = 0.32$  yielded the lowest RMSE in comparison to other Kanerva coder parameter choices, regardless of the choice of step size. In a second step, the RMSE for each GVF was calculated for each step size candidate, so the best step size for each GVF could be chosen independently. The best step sizes ranged from  $\frac{0.001}{n \cdot \eta}$  to  $\frac{0.256}{n \cdot \eta}$ , where the product  $n \cdot \eta$  is the number of active features.

The parameters that yielded the best performance in terms of RMSE for classic TD also performed best in the parameter sweep for TIDBD. For each feature, the step size was initialized to 0.00104, which corresponds to an initial value of  $\frac{1}{n \cdot \eta}$ . After the best parameters were established for classic TD and TIDBD, 30 independent trials were performed for each.

We programmed the robotic arm with a repeating series of periods of rest and periods of motion. The experiments started with the arm holding its position for five minutes. This period of rest was followed by five minutes of the arm repeating a complex pattern of movement that was programmed using a data glove. The movement pattern included motion of all joints and involved movements that humans with intact arms take for granted, like grasping or flexing one finger after another. For a better understanding, the exact movement pattern can be found online at [https://blinclab.ca/mpl\\_teleop\\_video/](https://blinclab.ca/mpl_teleop_video/). The movement pattern was 100 seconds long, so was repeated three times during the five-minute period of movement. The periods of rest and movement alternated three times, totalling 30 minutes.

During the rest period, each position, velocity and load sensor would be expected to report a constant signal, up to machine precision. Such sensor values should be easy to learn. During the movement pattern, on the other hand, the robot is in contact with human intention, so the predictions become far more difficult

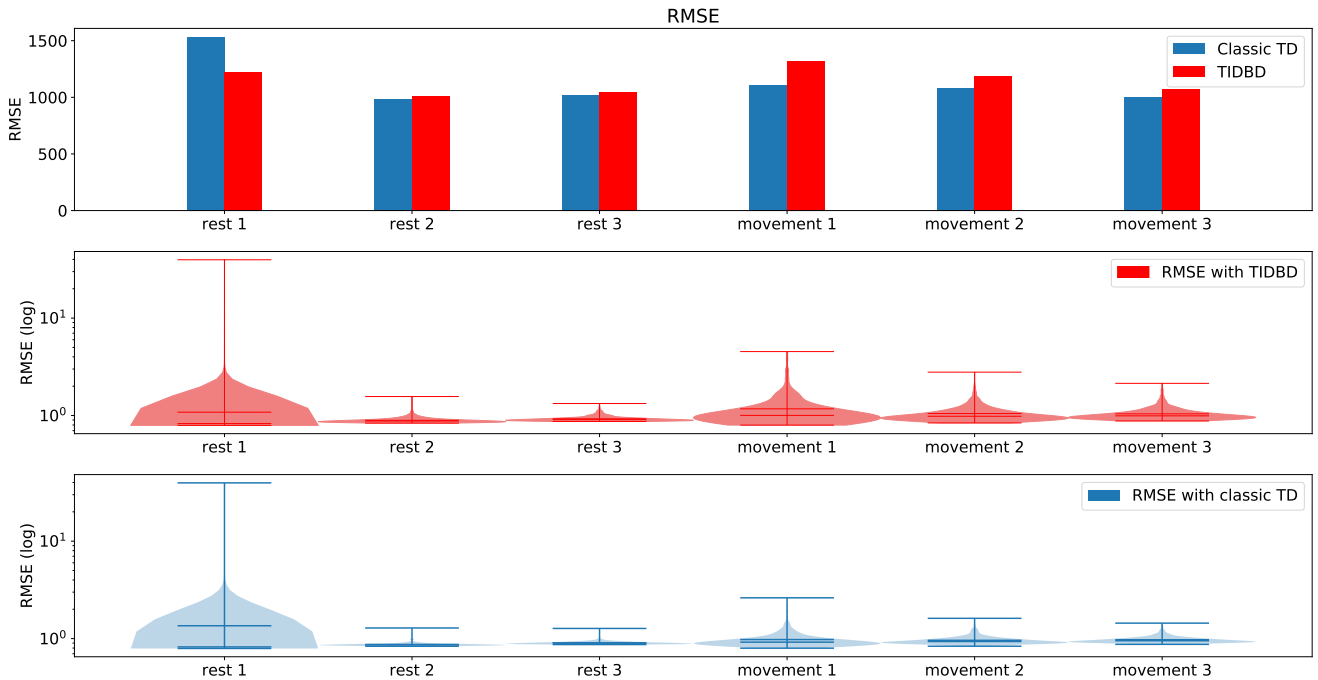


**Figure 3.** RMSE and violin plots for the experiment. The top pane shows the RMSE for both classic TD and TIDBD for each of the different time periods. The middle and bottom panes show violin plots for the RMSE, for TIDBD and classic TD respectively. All results are the average over 30 independent runs.

to make. The full series of periods of rest and movement provided an interesting test case, approximating intermittent stationarity and non-stationarity, to investigate the effect of TIDBD on GVF predictions.

Beyond our investigation of TIDBD with all sensors fully functioning, we also investigated how TIDBD reacts when confronted with two commonly occurring sensor failures: 1) sensors being stuck and 2) sensors being broken. A stuck sensor typically outputs a constant signal with a small amount of sensor noise (Li and Yang, 2012), while a broken sensor typically outputs Gaussian noise with a high variance (Ni et al., 2009). In both experiments, the signals from all four sensors in the elbow were replaced: in the first, with Gaussian noise of  $\mathcal{N}(1, 0.5)$  for the stuck sensors, and with Gaussian noise of  $\mathcal{N}(0, 10)$  for the broken sensors.

## 4 RESULTS AND DISCUSSION

The experiments were designed to investigate the effect that TIDBD has on predictions about the signals provided by a sensor-rich robotic arm. As a baseline, classic TD with an extensive parameter search was implemented. Three different scenarios were introduced: the predictions for different patterns of movement and rest, the predictions for the same patterns when the four elbow sensors are stuck and report a slightly noisy constant signal, and the predictions for the patterns when the four elbow sensors are broken and only report noise.

### 4.1 Comparison of Classic TD and TIDBD

We first consider the root mean squared error (RMSE, as defined in Section 3) for both classic TD and TIDBD in our initial experiment, where all sensors are fully functional. The top pane of Figure 3 shows the RMSE for each period of rest and movement. It can be seen that the highest error for both classic TD and

GVF setting	Fixed step size	TIDBD
Rest 1	1531.84	1222.90
Rest 2	983.72	1009.14
Rest 3	1023,00	1046.66
Movement 1	1105.32	1323.94
Movement 2	1085.81	1184.09
Movement 3	1003.21	1072.13

**Table 2.** Average RMSE over 30 independent runs

TIDBD occurs during the first period (Rest 1). This can easily be explained by all GVFs being initialized without any knowledge about the sensor readings—the RMSE for the first time steps will therefore be high. These high errors can be well seen in the violin plots, in the middle and bottom panes, which show the distribution over the errors the predictions made, the extrema, and the medians in the subplots for both classic TD and TIDBD. The maxima for TD and TIDBD were significantly higher in this period than for any other part of the experiment and the error distribution was much broader, as indicated by the colored area in the violin plots in Figure 3. Unsurprisingly, TIDBD exhibited a higher RMSE than classic TD at the beginning of the experiment, as its step sizes were initialized more aggressively and were not tuned to the predictive task.

The error for the second rest period was already significantly lower. Perhaps unintuitively, the error for the third rest period increased again. This can be explained by the sensor data from Figure 2. One of the load sensors started to drift in the third rest period. As this pattern had not been seen in any of the rest periods before, the RMSE peaked again—the pattern of a drifting sensor had not been learned, yet. For the periods of movement, a steady decrease in RMSE was observed.

On average, TIDBD had a slightly higher RMSE for the 30-minute experiment. It is important to recognize that our parameter sweep over step sizes provided an advantage to classic TD; because the step sizes were chosen to minimize the RMSE for the full experimental data, their choice inherently provided some information, which TIDBD did not receive, about the data. In a real-world application, providing this advantageous information in the form of parameters would not be possible, as the learner would be constantly faced with new, unknown data after the parameters have been set.

Despite this advantage, TIDBD and classic TD performed comparably with respect to the RMSE. This result indicates that TIDBD can act as an alternative to tuned classic TD learning, without the time- and labour-intensive setup that TD learning requires for tuning.

The choice of parameters appears to have a tremendous impact on the learning performance. Wrong parameters might result in almost no learning at all or constant overshooting. Adapting the parameters based on the incoming data should therefore result in better and more steady performance. To see whether TIDBD demonstrates more steady performance, we considered the sensitivity of the RMSE to the parameter settings for each algorithm. Our experimental data shows that classic TD was indeed strongly dependent on the learning rate: the standard deviation of the RMSE over the 264 combinations of parameters in our full factorial design was  $\sigma_{TD_{264}} = 43,734.46$ . In comparison, once the best step sizes for classic TD were preselected, the standard deviation for the remaining 24 experiments was  $\sigma_{TD_{24}} = 313.42$ . This value is over 100 times smaller than the standard deviation for all 264 experiments.

TIDBD, for which there are no learning rates to tune, attained a standard deviation of  $\sigma_{TIDBD} = 1,507.24$  over the 24 Kanerva coder parameters. This value is  $\sim 30$  times smaller than  $\sigma_{TD_{264}}$ , but  $\sim 5$  larger than

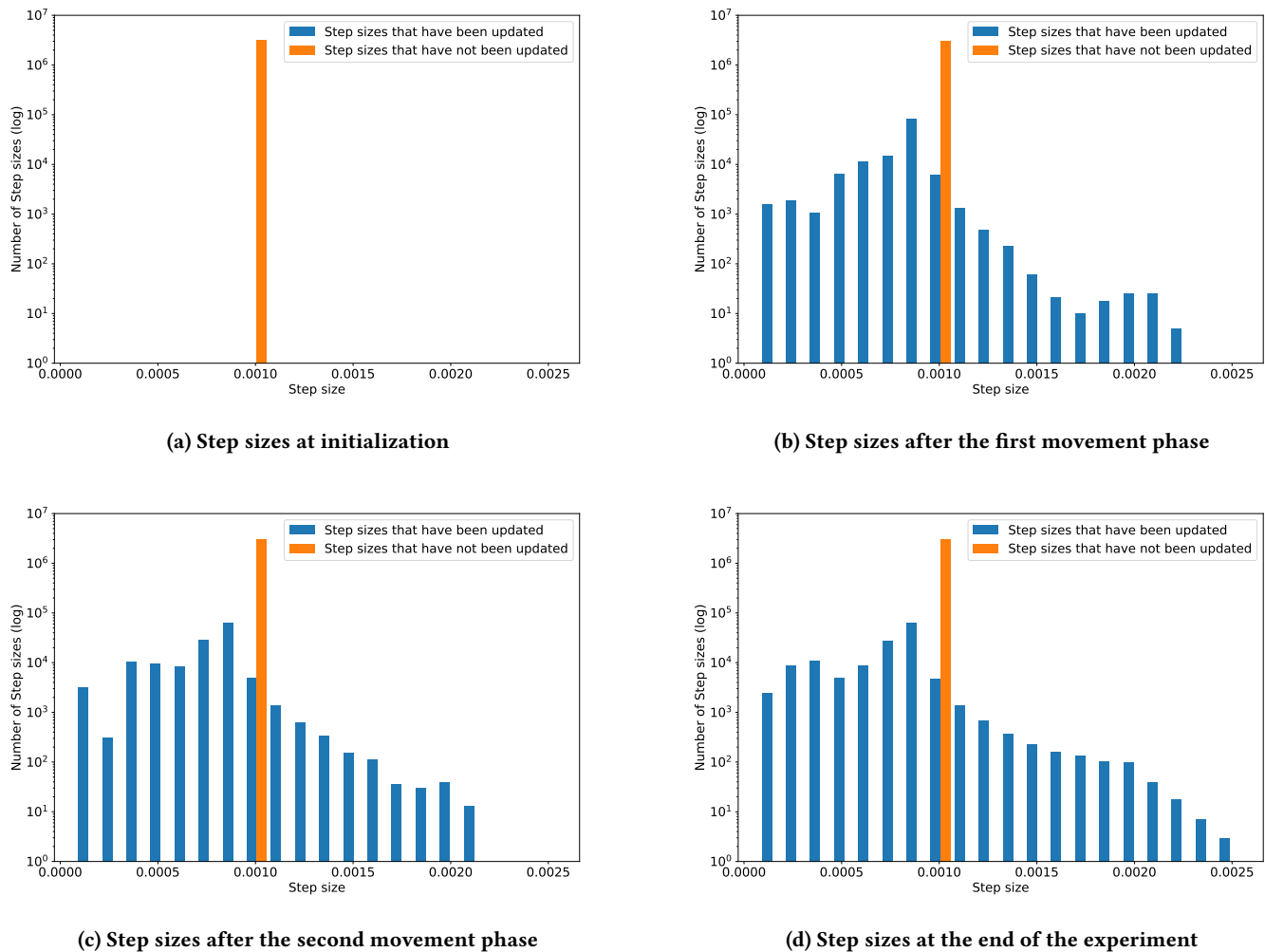


**Figure 4.** Step-size development over the course of the experiment. Each subplot shows the step-size distribution for a snapshot of the experiment. As TIDBD adapts the step sizes, this distribution will change.

$\sigma_{TD_{.24}}$ . The difference in the standard deviation between classic TD with a preselected learning rate and TIDBD is most likely due to the duration of the experiment. As classic TD was initialized with optimized step sizes, it was able to perform more effectively over a short period of time.

The above comparison of classic TD and TIDBD in terms of RMSE is valuable because it helps us understand the performance of TIDBD and demonstrates its potential for attaining similar performance to classic TD without a manual tuning process for the learning rate. However, feasibility also depends on computation and memory, and there is an associated cost with using TIDBD to update the step sizes without human interaction. For each weight in the 108 GVF, an additional step size was required. Given a feature representation with 30,000 features per GVF, 3,240,000 step sizes were required in this particular setting. Per GVF, three additional vectors of the same size as the number of features are required. In our Python implementation, each of the three additional weight vectors required 0.24 megabytes, totalling to an additional 0.72 megabytes. The additional computation for updating this larger number of step sizes increased the time for updating all GVFs from 0.025s to 0.28s. However, as this corresponds to nearly four updates per second, it was still within the requirement for a prosthetic limb.

The computations were performed using a Linux Mint 18.3 OS system with an i7-7700HQ CPU with a 3.80GHz clock rate, 6 MB of shared L3 cache and 32GB DDR4 RAM. With the ongoing evolution of

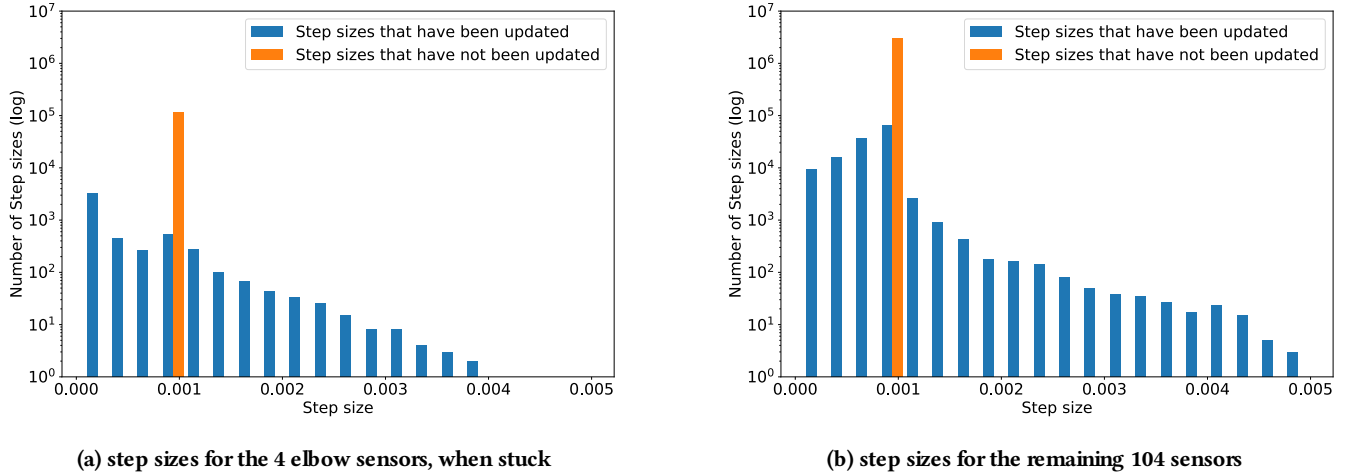


**Figure 5.** Step sizes distribution for the four elbow sensors (a) and the remaining 104 sensors (b), when the four elbow sensors are stuck.

hardware, we expect it to become possible to maintain and update even greater numbers of GVFs or to reduce the time needed for computation.

Our experimental data also offers us the opportunity to gain insight into the meta-learning process resulting from applying TIDBD. TIDBD assigns different step sizes to different GVFs and different features. As a result, different features contribute different amounts over time. Step sizes that are related to unimportant or noisy features will be reduced. These individual updates can be interpreted as a feature selection mechanism—TIDBD actively adapts its representation of the predictive problem, solely based on interactions with the environment (Kearney et al., 2019).

To better understand how TIDBD changes step sizes throughout the experiment, Figure 4 shows four snapshots of the distribution of the step sizes. In each subplot, the orange bar shows step sizes that had not yet been updated, due to the corresponding features not being activated; the blue bars represent the step sizes that had been updated by TIDBD. Subplot (a) shows the step sizes at initialization. All of the step sizes were initialized to 0.00104. As we would expect, Subplots (b), (c) and (d) show that the longer the experiment had run, the more the step sizes had spread out. Subplot (d) shows that the step sizes were set, by the end of the experiment, to within the range from  $8.0008 \times 10^{-5}$  to 0.00255.

Although TIDBD actively improves its representation by adapting the step sizes, it was still sensitive to the representation that was provided, as its performance significantly varied ( $\sigma_{TIDBD} = 1,507.24$ ) with the Kanerva coder parameters—information that is not provided to the learner due to an insufficient state representation cannot be compensated for. Within the realm of robotics, the state representation is often negatively impacted by damage to the sensors. We explore this problem in the following section by comparing the behaviour of TIDBD on data with simulated broken and stuck sensors with the behaviour demonstrated in the first experiment, shown in Figure 4.

## 4.2 Stuck Sensors

For the second experiment, recall that the elbow sensors were replaced with low-variance Gaussian noise,  $\mathcal{N}(1, 0.5)$ , to simulate them being stuck. The distribution of adapted step sizes at the end of this experiment can be found in Figure 5.

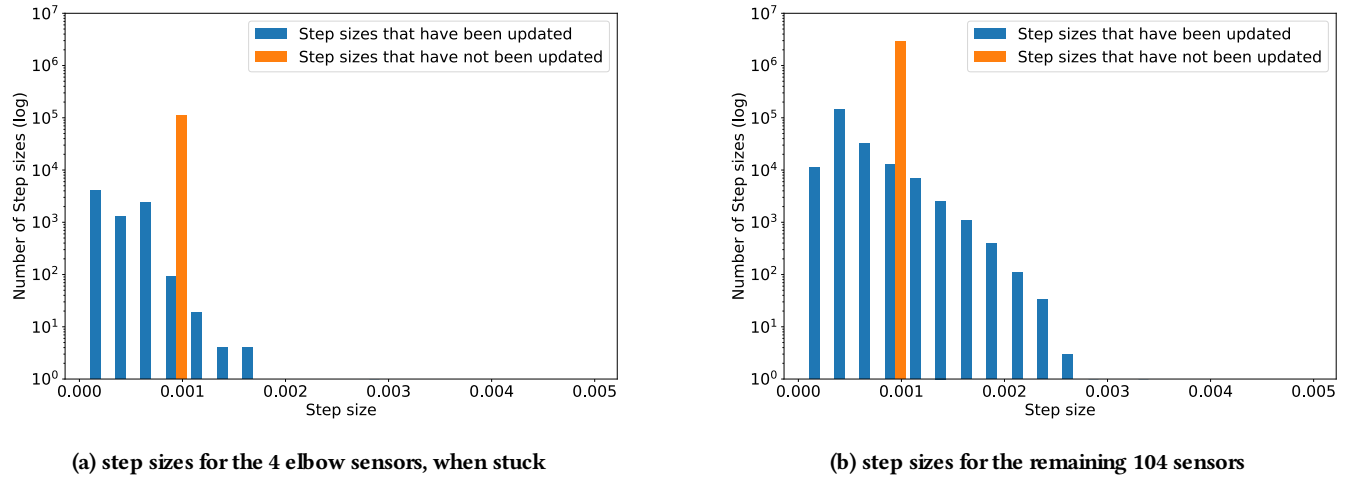


**Figure 6.** Step sizes distribution for the four elbow sensors (a) and the remaining 104 sensors (b), when the four elbow sensors are broken.

In comparing Figure 5 with Figure 4, of particular note is the fact that, with simulated stuck sensors, some step sizes were adapted to be much larger than any adapted during normal operation; the maximal step size when all sensors were functioning was 0.00255, while Figure 5 shows step sizes of up to 0.005, approximately twice as large.

The step sizes for both the predictions with stuck sensor signals as their cumulants *and* for the remaining “unaffected” predictions increased in magnitude. This result may be counterintuitive at first. For a constant signal with a small amount of noise, we would expect the step sizes to decrease, as such a signal does not contain a significant amount of information. In the setting at hand, this reaction is countered by the choice of representation. As the Kanerva coder prototypes were randomly distributed in space, the small amount of noise could actually be expected to constantly lead to different prototypes being activated. At the same time, the cumulants were staying nearly constant, due to the variance being small. This discrepancy between almost stationary cumulants and a changing representation appears to have led to increasing step sizes, as TIDBD tried to achieve the necessary updates in fewer steps. Each feature was assigned a higher value, likely due to these updates being distributed over a wider range of features, resulting in higher step sizes. While these increasing step sizes did not necessarily improve the representation, they are clearly distinguishable from step sizes that occurred during the normal functioning of the robotic arm, thus providing important knowledge about the sensor failure.

### 4.3 Broken Sensors

The problem of broken sensors is a common one in robotics and of high interest in long-term autonomous systems. For the final experiment, the four elbow sensors were replaced with Gaussian noise,  $\mathcal{N}(0, 10)$ , which corresponds to broken sensors that output noise. Such broken sensors do not contain meaningful information, as their output will be purely random—we therefore expect TIDBD to decrease the corresponding step sizes for these sensors. Figure 6 shows the step size distribution for the experiment with broken sensors that output high-variance noise drawn from  $\mathcal{N}(0, 10)$ . Subplot (a) depicts the step-size distribution for the four sensors that output noise. The maximum step size is only 0.0017. The step sizes observed during this experiment were significantly smaller than they were in the experiments where all sensors function well. The average step size for the broken sensors is 0.00037, while the average step size for these four sensors in the experiment with functioning sensors is 0.00065. Subplot (b) shows the

distribution for the remaining 104 sensors. While the maximum in this experiment, with a value of 0.0028, was almost identical to the maximum of 0.0025 in the experiment where all sensors work well, there is a significant distinction in the average step sizes. For the experiment with broken sensors, the average step size was 0.0006, while it was 0.00077 in the experiment where all of the sensors are functioning as expected. The RMSE for the 104 functioning sensors, given broken elbow sensors, was calculated for both a TIDBD Horde and a classic TD Horde. The information provided by the elbow sensors was used in the feature representation  $\mathbf{x}(s)$ , but since these sensors are broken, they only provided irrelevant, distracting information to the predictors. For the classic TD Horde, the RMSE for the 104 functioning sensors increased to 1,315,850.16. Step-size adaptation using TIDBD resulted in a significantly lower RMSE of 509,220.75.

As expected, the step sizes corresponding to the four sensors that were replaced by noise were significantly decreased when compared to the step sizes during normal operation. Based on the interaction with these sensors, TIDBD appears to decide that it cannot learn additional information about them and to exclude them from further learning. The step sizes for the remaining 104 sensors remained almost the same as in the normal operation of the arm. However, the distribution of step sizes in the intact sensors changed slightly as more step sizes were decreased in value—potentially to exclude features that correspond to the noisy inputs from impacting the predictions about the functioning sensor values. The RMSE for the remaining 104 sensors supports this intuition, as it is  $\sim 2.5$  times lower (1,315,850.16 for classic TD vs. 509,220.75 for TIDBD) for TIDBD than for classic TD.

Together, the results in this paper not only support the usability of TIDBD to independently learn and update step sizes for predictions without the need of human assistance, but furthermore to independently adapt the representation that is used for a predictive knowledge approach. As TIDBD updates the step sizes based solely on interactions with the environment and grounded in the observations that are received from said environment, it can truly function on its own—even when implemented in a long-lived application.

## 5 CONCLUSION

The experiments in this paper were conducted to investigate TIDBD—a step-size adaptation algorithm that assigns individual step sizes on the feature level. Three different experiments were performed on a sensor-rich robotic arm to gain further insight into the functioning of TIDBD. All three experiments utilize the data from alternating patterns of rest and movement.

**First experiment:** We compared the predictive performance of classic TD with an extensive parameter search with that of TIDBD. The additional computation required by TIDBD was still within our requirements for real-time and the memory used for TIDBD is negligible on modern systems. The results show that TIDBD performed comparably to classic TD in terms of the root mean squared error (RMSE), thus rendering an extensive learning rate parameter search needless.

**Second experiment:** We then explored the changes in the learning rates with several stuck sensors. The changes in the TIDBD step sizes were clearly distinguishable from changes seen during normal functioning of the arm (as explored in the first experiment), therefore providing an indicator to detect this type of sensor failure.

**Third experiment:** We replaced several sensors with high variance noise, simulating broken sensors. TIDBD decreased the step sizes corresponding to the broken sensors, which resulted in these inputs being gradually excluded from the updates—it automatically learned the unimportance of these inputs.

These three results—the permanent updates of step sizes to accommodate non-stationarity, the distinct reaction to stuck sensors, and the automatic feature selection for uninformative sensors—are promising key features for long-term autonomous agents. They empower an agent to not only adapt its learning based on interactions with its environment, but to evaluate and improve its own perception of said environment.

Furthermore, as the step sizes contain information about the past for each feature, they can provide an important source of information to the agent itself to learn from. As has been argued prior to this work (Schultz and Dickinson, 2000; Sherstan et al., 2016; Günther et al., 2018), these introspective signals provide a helpful source of information to enable an agent to better understand its environment and its own functioning within its environment

The insights presented in this paper provide deeper understanding and intuition about the effects of TIDBD, aiming to help other designers in creating agents that are capable of autonomous learning and adaptation through interaction with their environment.

## ACKNOWLEDGEMENTS

This research was undertaken, in part, thanks to funding from the Canada Research Chairs program, the Canada Foundation for Innovation, the Alberta Machine Intelligence Institute, Alberta Innovates, and the Natural Sciences and Engineering Research Council. The authors also thank Jaden Travnik for discussions on Kanverva coding and Craig Sherstan as well as Richard Sutton for suggestions and helpful discussions.

## REFERENCES

- Bridges, M. M., Para, M. P., and Mashner, M. J. (2011). Control system architecture for the modular prosthetic limb. *Johns Hopkins APL Technical Digest* 30, 217–222
- Dalrymple, A. N., Everaert, D. G., Sutton, R. S., and Mushahwar, V. K. (2018). Online prediction of phases of the gait cycle for control of intraspinal microstimulation. In *Society for Neuroscience*
- Drescher, G. L. (1991). *Made-Up Minds: A Constructivist Approach to Artificial Intelligence* (MIT press)
- Edwards, A. L., Dawson, M. R., Hebert, J. S., Sherstan, C., Sutton, R. S., Chan, K. M., et al. (2016). Application of real-time machine learning to myoelectric prosthesis control: A case series in adaptive switching. *Prosthetics and orthotics international* 40, 573–581
- Günther, J., Kearney, A., Dawson, M. R., Sherstan, C., and Pilarski, P. M. (2018). Predictions, surprise, and predictions of surprise in general value function architectures. In *AAAI Fall Symposium*. 8
- Günther, J., Pilarski, P. M., Helfrich, G., Shen, H., and Diepold, K. (2016). Intelligent laser welding through representation, prediction, and control learning: An architecture with deep neural networks and reinforcement learning. *Mechatronics* 34, 1–11
- Kahn, G., Villaflor, A., Ding, B., Abbeel, P., and Levine, S. (2018). Self-supervised deep reinforcement learning with generalized computation graphs for robot navigation. In *Proceedings of the International Conference on Robotics and Automation (IEEE)*, 1–8
- Kearney, A., Veeriah, V., Travnik, J., Pilarski, P. M., and Sutton, R. S. (2019). Learning feature relevance through step size adaptation in temporal-difference learning. *arXiv preprint arXiv:1903.03252*
- Li, X.-J. and Yang, G.-H. (2012). Fault detection for linear stochastic systems with sensor stuck faults. *Optimal control applications and methods* 33, 61–80
- Mahmood, A. R., Sutton, R. S., Degris, T., and Pilarski, P. M. (2012). Tuning-free step-size adaptation. In *Proceedings of the International Conference on Acoustics, Speech and Signal Processing (IEEE)*, 2121–2124

- Modayil, J. and Sutton, R. S. (2014). Prediction driven behavior: Learning predictions that drive fixed responses. In *Workshops at the Twenty-Eighth AAAI Conference on Artificial Intelligence*
- Modayil, J., White, A., and Sutton, R. S. (2014). Multi-timescale nexting in a reinforcement learning robot. *Adaptive Behavior* 22, 146–160
- Ni, K., Ramanathan, N., Chehade, M. N. H., Balzano, L., Nair, S., Zahedi, S., et al. (2009). Sensor network data fault types. *ACM Transactions on Sensor Networks (TOSN)* 5, 25
- Pilarski, P. M., Dawson, M. R., Degris, T., Carey, J. P., Chan, K. M., Hebert, J. S., et al. (2013). Adaptive artificial limbs: A real-time approach to prediction and anticipation. *IEEE Robotics & Automation Mag.* 20, 53–64
- Pilarski, P. M., Sutton, R. S., Mathewson, K. W., Sherstan, C., Parker, A. S., and Edwards, A. L. (2017). Communicative capital for prosthetic agents. *arXiv preprint arXiv:1711.03676*
- Ring, M. B. (1994). *Continual Learning in Reinforcement Environments*. [PhD Thesis], [Austin (TX)]: University of Texas at Austin
- Schlegel, M., White, A., Patterson, A., and White, M. (2018). General value function networks. *arXiv:1807.06763 [cs, stat]*
- Schultz, W. and Dickinson, A. (2000). Neuronal coding of prediction errors. *Annual Review of Neuroscience* 23, 473–500
- Sherstan, C., Machado, M. C., and Pilarski, P. M. (2018). Accelerating learning in constructive predictive frameworks with the successor representation. *arXiv preprint arXiv:1803.09001*
- Sherstan, C., Modayil, J., and Pilarski, P. M. (2015). A collaborative approach to the simultaneous multi-joint control of a prosthetic arm. In *Proceedings of the International Conference on Rehabilitation Robotics (IEEE)*, 13–18
- Sherstan, C., White, A., Machado, M. C., and Pilarski, P. M. (2016). Introspective agents: Confidence measures for general value functions. In *Proceedings of the International Conference on Artificial General Intelligence (Springer)*, 258–261
- Sinclair, A. H. and Barense, M. D. (2018). Surprise and destabilize: Prediction error influences episodic memory reconsolidation. *Learning & Memory* 25, 369–381
- Sutton, R. S. (1988). Learning to predict by the methods of temporal differences. *Machine learning* 3, 9–44
- Sutton, R. S. (1992). Adapting bias by gradient descent: An incremental version of delta-bar-delta. In *AAAI*. 171–176
- Sutton, R. S. and Barto, A. G. (2018). *Reinforcement Learning: An Introduction* (MIT press)
- Sutton, R. S., Modayil, J., Delp, M., Degris, T., Pilarski, P. M., White, A., et al. (2011). Horde: A scalable real-time architecture for learning knowledge from unsupervised sensorimotor interaction. In *Proceedings of the International Conference on Autonomous Agents and Multiagent Systems-Volume 2 (AAMAS)*, 761–768
- Travnik, J. B. (2018). *Reinforcement Learning on Resource Bounded Systems*. Master’s thesis, University of Alberta
- Travnik, J. B. and Pilarski, P. M. (2017). Representing high-dimensional data to intelligent prostheses and other wearable assistive robots: A first comparison of tile coding and selective Kanerva coding. In *Proceedings of the International Conference on Rehabilitation Robotics (IEEE)*, 1443–1450
- White, A. (2015). *Developing a Predictive Approach to Knowledge*. [PhD Thesis], [Edmonton (AB, Canada)]: University of Alberta